Case Series: Clinical Application in Liver Fat and Iron Quantification using LiverLab

Barbara Frittoli, M.D.[1]; Martina Bertuletti, M.D.[1]; Valentina Angelini, M.D.[2]; Luigi Grazioli, M.D.[1]

[1]ASST-Spedali Civili di Brescia, Italy
[2]"Federico II" University, Naples, Italy

Background

In western countries in the last ten years, nonalcoholic fatty liver disease (NAFLD) has increased in incidence and prevalence, as has its advanced form, nonalcoholic steatohepatitis (NASH). These are complex metabolic alterations of liver function and structure. They have long term impacts on health and quality of life, raising the risk of cirrhosis and hepatocellular carcinoma. In the USA they are now the second indication for liver transplantation [1–5].

It has therefore become necessary to characterize and quantify the liver reversible modifications such as intrahepatic fat and iron overload associated with NAFLD and NASH. The ability to quantify liver fat will also benefit patients with chemotherapy-associated-steatohepatitis (CASH); and quantifying iron accumulation can benefit those with hemochromatosis, hemosiderosis, and chronic hepatopathy diseases [1–5].

These overload diseases usually have heterogeneous distribution within the liver, which is a challenge for liver biopsy. Biopsy is still considered by clinicians as the gold standard for diagnosis and quantification, despite being invasive. However, biopsy does not always show the real severity of the disease and its distribution within the parenchyma because it samples only one or a few sites.

Various noninvasive qualitative and quantitative techniques can be used to quantify liver steatosis, including ultrasound and computed tomography; but MRI is the most accurate and reproducible technique. MRI is also the only accurate method for detecting iron overload in the liver.

In recent years, software has been developed to automatically manage quantitative measurements and represent them with color parametric maps, which has simplified the use of quantitative MR imaging in everyday clinical practice [6].

Recent MRI methods for liver fat and iron quantification in the liver are based on the Dixon technique and spectroscopy. These methods are available as LiverLab on our magnetic resonance tomographs 1.5T MAGNETOM Aera and 3T MAGNETOM Skyra (Siemens Healthcare, Erlangen, Germany).

LiverLab comprises a fat and iron screening component (two-point e-Dixon), and two methods for evaluation: multi-echo Dixon VIBE (six point q-Dixon), an image-based method; and HISTO, a voxel-based spectroscopic method. It also provides clinical reports. In our experience with LiverLab, we take advantage of its very fast acquisition, reproducibility of results and interpretation immediacy [7–8].
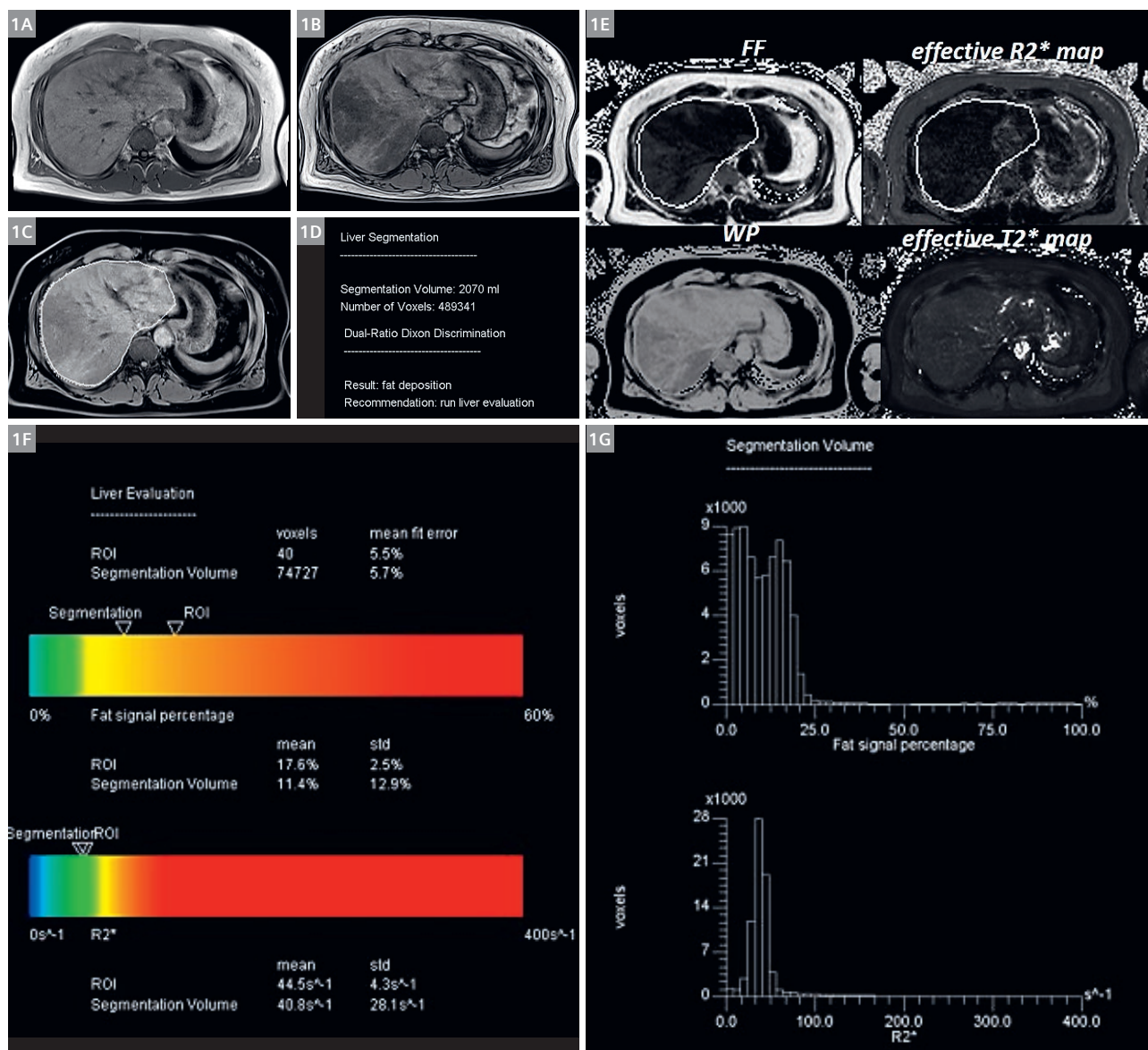
For our patients undergoing MR liver examination, the first sequences acquired during our liver protocol are T1 GRE in/opp. If liver signal intensity is hypointense in in-phase or opposed-phase acquisition, LiverLab is acquired before contrast media administration, in order to identify and quantify fat and/or iron deposition. It takes about 5–7 minutes if both Multi-echo Dixon VIBE and HISTO are acquired, and doesn't alter the regular workflow. Some hepatopathic and hematological patients are scheduled only for LiverLab acquisition by Hepatologists and Hematologists and then the complete MR examination takes about 10 minutes, with T2* map added to the protocol.

In our experience, LiverLab has become routinely useful in evaluating liver overload diseases in many clinical assets, bringing the advantages of rapid, accurate and reproducible acquisition. Here we show examples, in patients with fat accumulation (NAFLD/NASH, liver chronic hepatopathy, CASH in oncological patients), iron accumulation (hemochromatosis, hemosiderosis), and both (NAFLD/chronic hepatopathy). This technique is useful for follow-up and drugs effect monitoring, due to easy and rapid administration and accurate measurement.

Case 1

50-year-old male with incidental finding of cholestasis and hypercholesterolemia. Ultrasound examination of the liver had very heterogeneous aspect, with hyperechoic areas and pseudonodular hypoechoic areas. The patient was scheduled for an MRI examination to quantify steatosis and characterize pseudonodular lesions. Images were acquired by 1.5T MAGNETOM Aera.
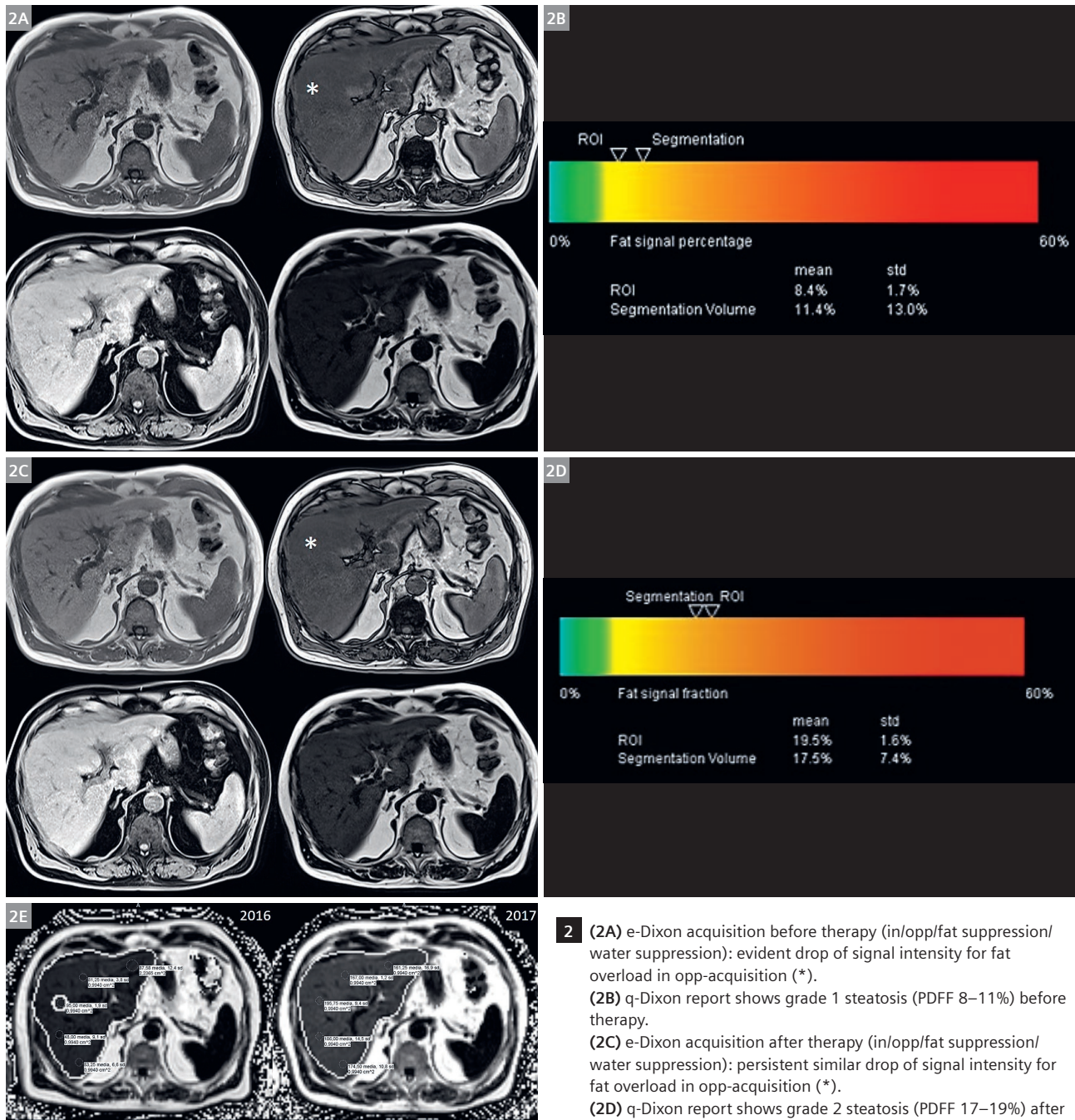
1D
Liver Segmentation

Segmentation Volume: 2070 ml
Number of Voxels: 489341

Dual-Ratio Dixon Discrimination

Result: fat deposition
Recommendation: run liver evaluation

1E
FF   effective R2* map
WP   effective T2* map

1F
Liver Evaluation
....

	voxels	mean fit error
ROI	40	5.5%
Segmentation Volume	74727	5.7%

Segmentation   ROI
0%   Fat signal percentage   60%

	mean	std
ROI	17.6%	2.5%
Segmentation Volume	11.4%	12.9%

SegmentationROI
0s^-1   R2*   400s^-1

	mean	std
ROI	44.5s^-1	4.3s^-1
Segmentation Volume	40.8s^-1	28.1s^-1

1G
Segmentation Volume

1 **(1A)** T1w GRE in-phase: liver of regular volume and morphology.
(1B) T1w GRE opp-phase: heterogeneous drop of signal within the liver parenchyma, in particular in the right lobe where some hypointense areas have pseudonodular aspect.
(1C) e-Dixon automatic liver segmentation.
(1D) e-Dixon report estimates liver volume and number of voxels, and reports the presence of intrahepatic fat.
(1E) Four of the five series of images from q-Dixon acquisition: FF (Fat Fraction), WF (Water Fraction), effective R2*, effective T2*.
(1F) q-Dixon report: color bars show the values of PDFF and R2* both for the whole liver volume segmented and for the ROI positioned in the right lobe. ROI value for PDFF is higher (17.6%) than segmentation value (11.4%) because of major fat accumulation in right lobe. Classification is grade 1–2 steatosis; R2* values are normal; no iron overload is detected.
(1G) q-Dixon report: histograms describe PDFF values and R2* values distribution.

Case 2

56-year-old male with steatosis. The patient was enrolled in a double-blind study in which steatosis was quantified by LiverLab performed on 3T MAGNETOM Skyra, before and after one year of therapy (drug versus placebo).

Qualitative imaging (in/opp or e-Dixon) could not correctly identify variation in fat overload; quantitative imaging (q-Dixon) could identify and measure PDFF before and after drug/placebo administration.

2 **(2A)** e-Dixon acquisition before therapy (in/opp/fat suppression/water suppression): evident drop of signal intensity for fat overload in opp-acquisition (*).
(2B) q-Dixon report shows grade 1 steatosis (PDFF 8–11%) before therapy.
(2C) e-Dixon acquisition after therapy (in/opp/fat suppression/water suppression): persistent similar drop of signal intensity for fat overload in opp-acquisition (*).
(2D) q-Dixon report shows grade 2 steatosis (PDFF 17–19%) after therapy.
(2E) q-Dixon FF series before and after therapy: multiple ROIs positioned in right liver lobe confirm PDFF values reported on colored bars.

Case 3

48-year-old female with single liver metastasis in S4 in obese patient with rectal cancer studied by MRI. The patient underwent chemotherapy and repeat MRI after three months to evaluate response to therapy: partial response was assessed but steatosis worsened and the patient could not go on with chemotherapy because of CASH. The multidisciplinary team decided to perform surgery "liver-first". The pathologic examination of liver surrounding resected metastasis confirmed grade 2 steatosis.
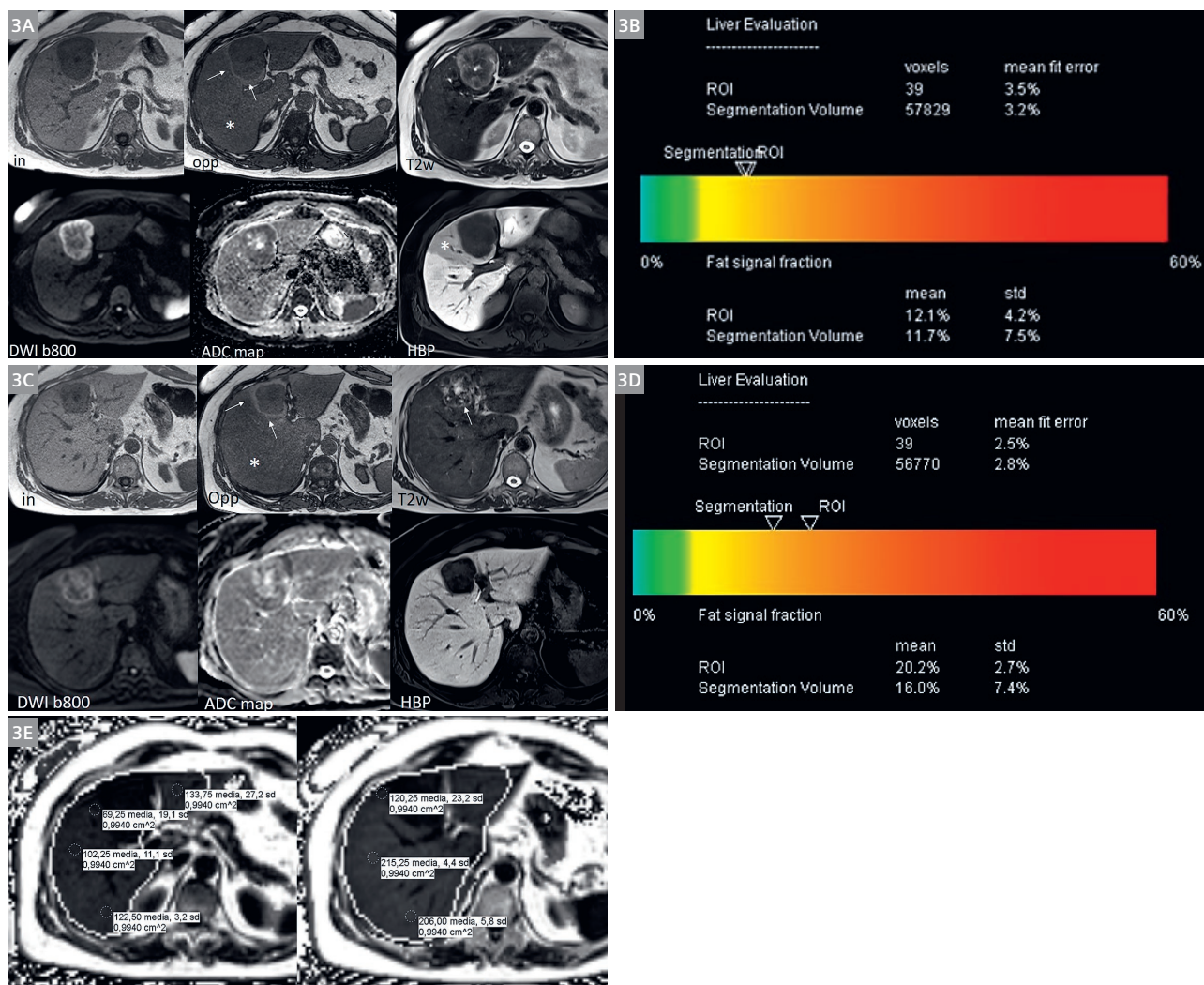
3 **(3A)** in-/opp, T2w, DWI (b800), ADC and hepatobiliary phase (HBP 15 min after EOB-DTPA injection) of the hepatic lesion at the initial staging: liver diffuse steatosis (* in opp); the lesion determines compression on left portal branch with consequent perilesional steatosis spare (arrows) and functional liver impairment (* in HBP).
(3B) q-Dixon report shows grade 1 steatosis (PDFF 11–12%) before chemotherapy.
(3C) in-/opp, T2w, DWI, ADC and HBP (15 min after EOB-DTPA injection) of the hepatic lesion after chemotherapy: liver diffuse steatosis persists (* in opp); the lesion is smaller but perilesional steatosis spare is still evident (arrows in opp); the signal of the lesion in T2w sequence is more heterogeneous (arrow) without any restriction of signal on DWI/ADC. The functional liver impairment is no easier to see during HBP.
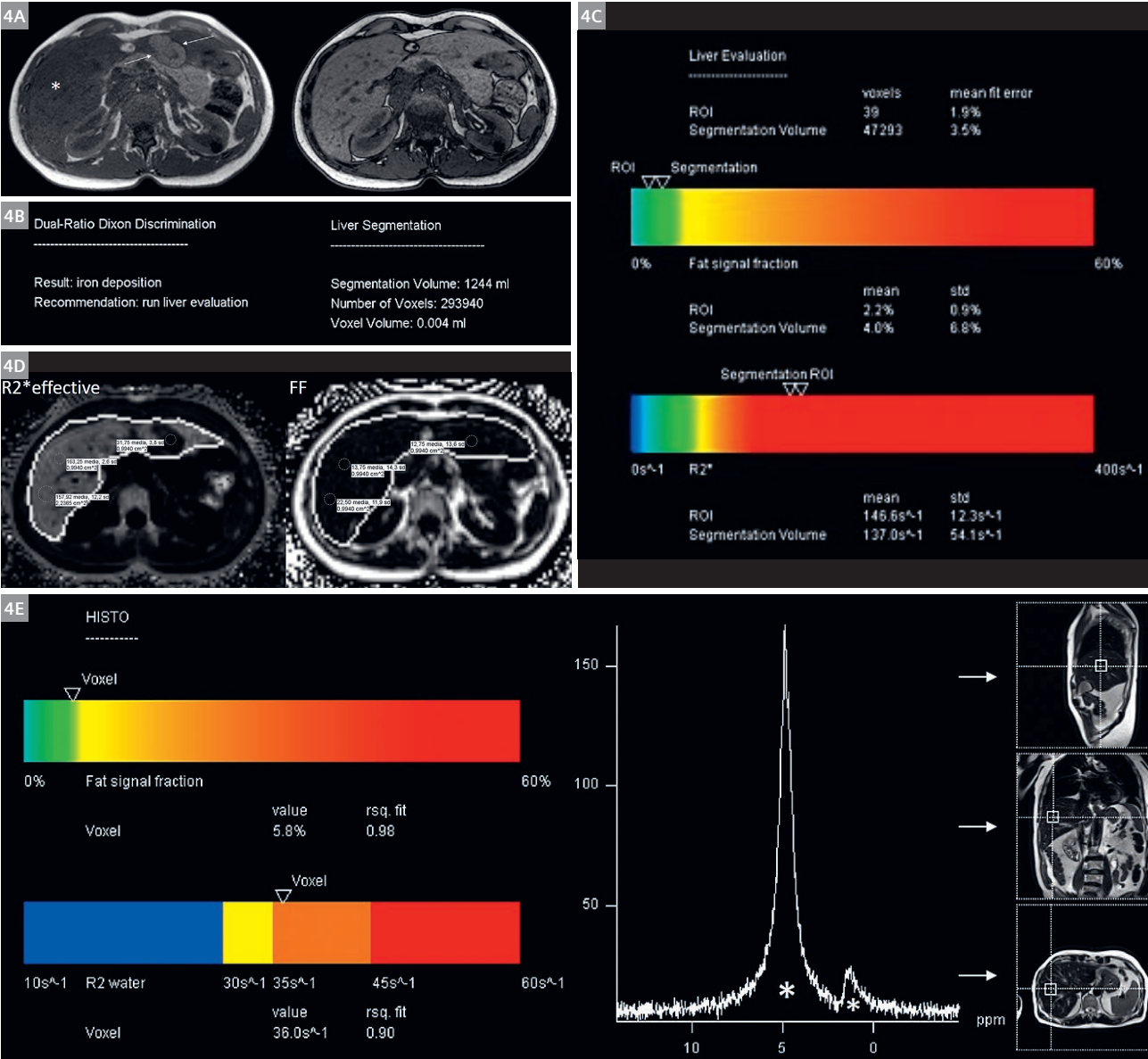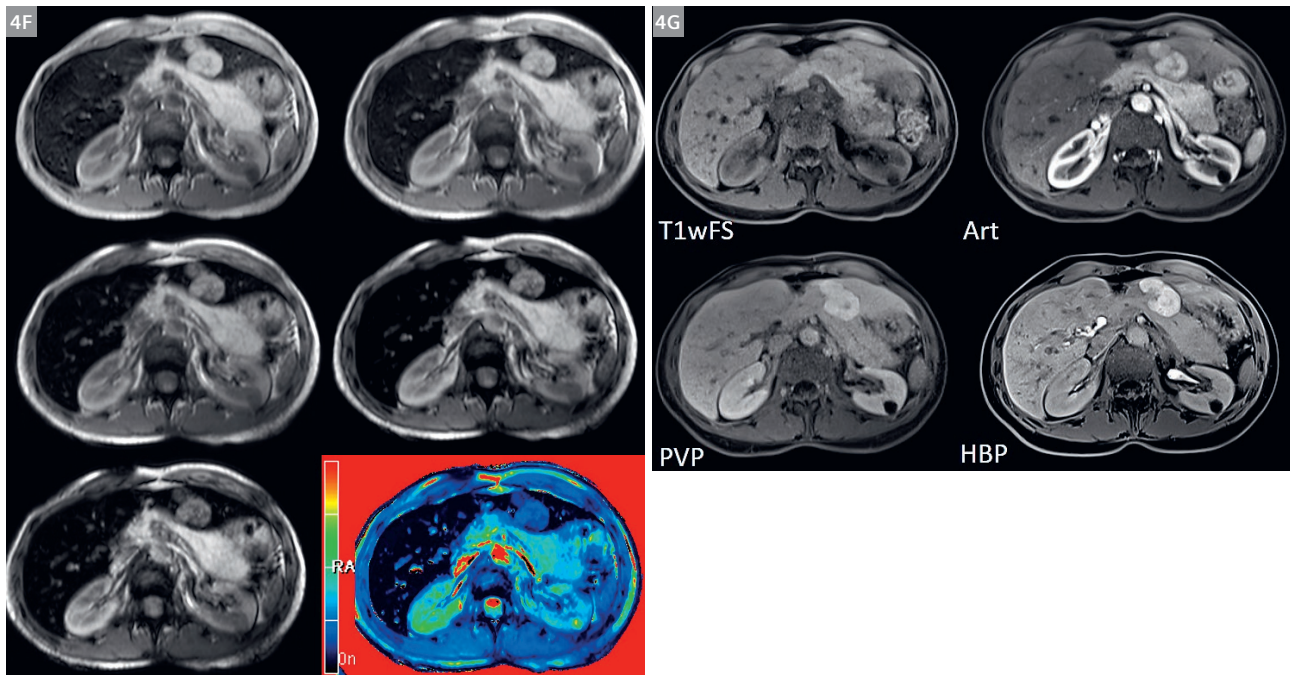**(3D)** q-Dixon report shows worsening of steatosis (grade 2, PDFF 16–21%) after chemotherapy.
(3E) q-Dixon FF series before and after (*) therapy: multiple ROIs in right liver lobe confirm PDFF values reported on colored bars of q-Dixon report.

Case 4

43-year-old female with incidental ultrasound finding of hypoechoic lesion in left lobe in hyperechoic liver – suspected steatosis. The patient was scheduled for MRI. With T1 GRE in/opp sequences, more hypointense signal of liver parenchyma was noted on T1 in-phase sequence. LiverLab was performed, and confirmed mild iron overload

(LIC 4.4–4.7 mgFe/g). The lesion in the left lobe had signal intensity and pattern of enhancement typical for focal nodular hyperplasia (FNH). The patient was given specific blood tests, and heterozygosis for hemochromatosis was confirmed.

4A

4B Dual-Ratio Dixon Discrimination

Result: iron deposition
Recommendation: run liver evaluation

Liver Segmentation

Segmentation Volume: 1244 ml
Number of Voxels: 293940
Voxel Volume: 0.004 ml

4C

Liver Evaluation

	voxels	mean fit error
ROI	39	1.9%
Segmentation Volume	47293	3.5%

0%   Fat signal fraction   60%

	mean	std
ROI	2.2%	0.9%
Segmentation Volume	4.0%	6.8%

0s^-1   R2*   400s^-1

	mean	std
ROI	146.6s^-1	12.3s^-1
Segmentation Volume	137.0s^-1	54.1s^-1

4D R2*effective   FF

4E HISTO

0%   Fat signal fraction   60%

	value	rsq. fit
Voxel	5.8%	0.98

10s^-1   R2 water   30s^-1 35s^-1   45s^-1   60s^-1

	value	rsq. fit
Voxel	36.0s^-1	0.90

4 **(4A)** T1 GRE in/opp sequence: the signal intensity of liver parenchyma is lower in in-phase acquisition (*); in the left lobe an exophytic lesion shows as isointense in opp-phase and hyperintense in in-phase (arrows).

(4B) e-Dixon report confirms iron overload and provides an estimation of liver volume.

(4C) q-Dixon report shows mild iron overload, with R2* of 137–147 sec^{-1}, corresponding to LIC of 4.4–4.7 mgFe/g. PDFF is normal (<5%).

(4D) q-Dixon R2*effective and FF sequences: multiple ROIs in right liver lobe confirm R2* and PDFF values reported on colored bars. No fat or iron overload can be detected within the lesion in the left lobe.

(4E) HISTO acquisition report confirms iron overload (R2 water 36 sec^{-1}; normal values <30 sec^{-1}) in the single voxel measured in right lobe (arrows indicate the site of the measured voxel in multiplanar vision). Asterisks represent T2-corrected peak areas for water and fat at each measured TE.

(4F) T2* multi-echo acquisition (TE = 9,53 – 14,29 – 19,05 – 23,81 and 28,58 seconds) and T2* colored map.

(4G) Characterization of the liver lesion before (T1w FatSat) and after contrast media administration (EOB-DTPA) during dynamic (arterial and portal venous phase) and hepatobiliary phase (HBP): focal nodular hyperplasia (FNH).

Case 5

68-year-old female with hemosiderosis. The patient undergoes MRI (LiverLab) to quantify iron overload and evaluate whether chelation therapy should be performed. After seven bloodletting sessions the patient was scheduled for LiverLab acquisition, which showed reduction of iron overload. Mild steatosis was associated with iron overload, and fat accumulation was reduced after therapy.
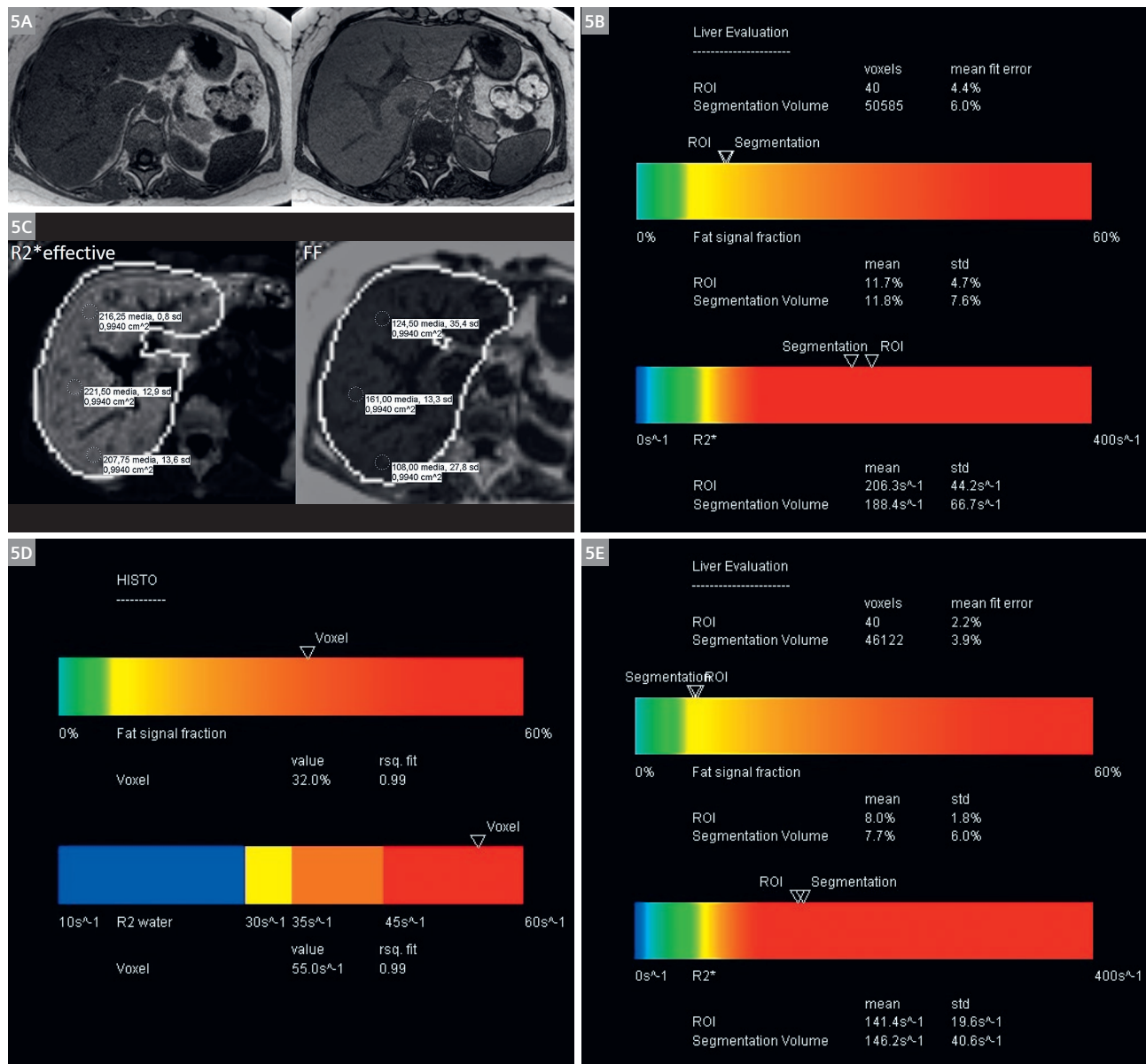
5 **(5A)** T1 GRE in/opp sequences
(5B) q-Dixon report shows iron overload, with R2* of 190–206 sec^{-1}, corresponding to LIC of 6.1–6.6 mgFe/g; and mild steatosis (PDFF 11–12%).
(5C) q-Dixon R2*effective and FF series: multiple ROIs positioned in right liver lobe confirm high R2* values (up to 221 sec^{-1}) and heterogeneous mild steatosis (PDFF 10–16%).
**(5D)** HISTO acquisition report confirms iron overload and steatosis: R2 water 55 sec^{-1} (normal values < 30 sec^{-1}) in the single voxel measured in right lobe. PDFF is 32% in the same voxel. According to literature, steatosis can be overestimated in presence of iron overload [14].
(5E) After bloodletting therapy, q-Dixon acquisitions demonstrate reduction in iron overload and steatosis: R2* is 145 sec^{-1}, corresponding to LIC of 4.64 mgFe/g. Steatosis is reduced (PDFF 7–8%).
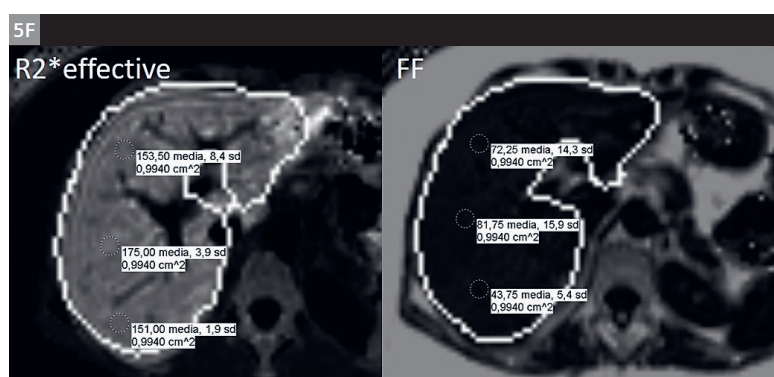
(5F) q-Dixon R2*effective and FF series: multiple ROIs in right liver lobe confirm high R2* values (up to 175 sec^{-1}) and mild steatosis (PDFF 7–8%) with areas of relative spare (PDFF 4.3% in S6).
(5G) HISTO confirms the effect of the therapy: R2 water is 50.7 sec^{-1} (normal values < 30 sec^{-1}) in the single voxel measured in right lobe. PDFF is 15% in the same voxel.
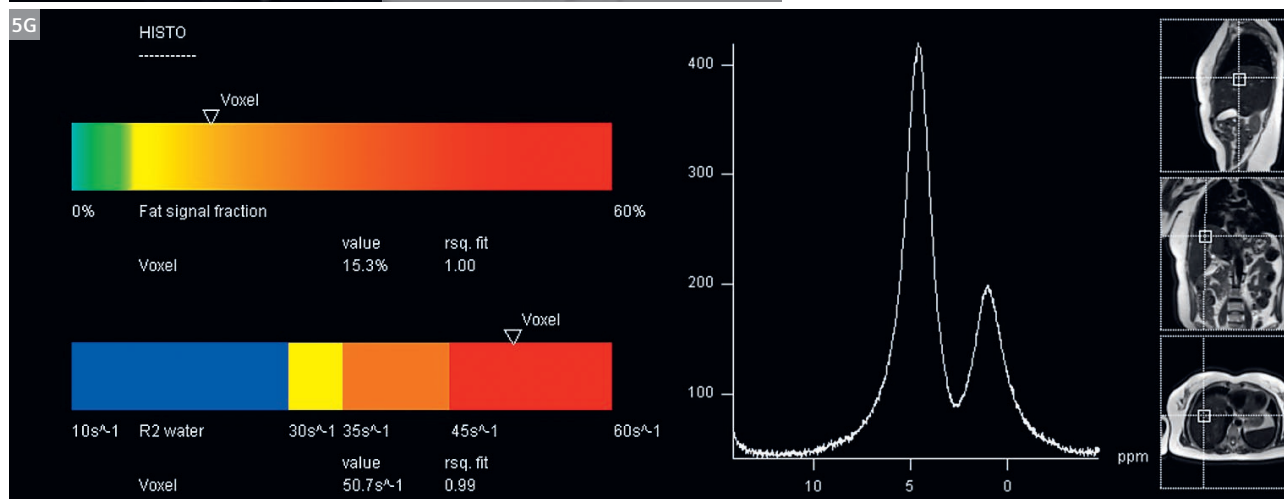
Technique

The first sequence is an e-Dixon, obtained in a single 15–20 second breath-hold acquisition, which returns four series of images: in/opp/fat suppression/water suppression. It gives a semi-quantitative evaluation of fat and iron buildup by estimating the total number of voxels (and the volume in mL of the hepatic parenchyma) and the presence of fat and/or iron in the parenchyma.

The six-point acquisition q-Dixon, obtained in a 18–20 second breath-hold acquisition, is a 3D multi-echo gradient echo sequence with Dixon reconstructions and correction for T2* in the presence of iron. It returns five series of images: FF (fat fraction), WF (water fraction), effective R2*, effective T2* and goodness-of-fit map for quality control. It also plots the distribution of measured echo times, and gives a graphical representation with color bars or colorimetric maps of the two biomarkers: PDFF (proton density fat fraction) and R2 * (1/T2*), both as average values calculated over the entire liver volume and as single voxel measurements.
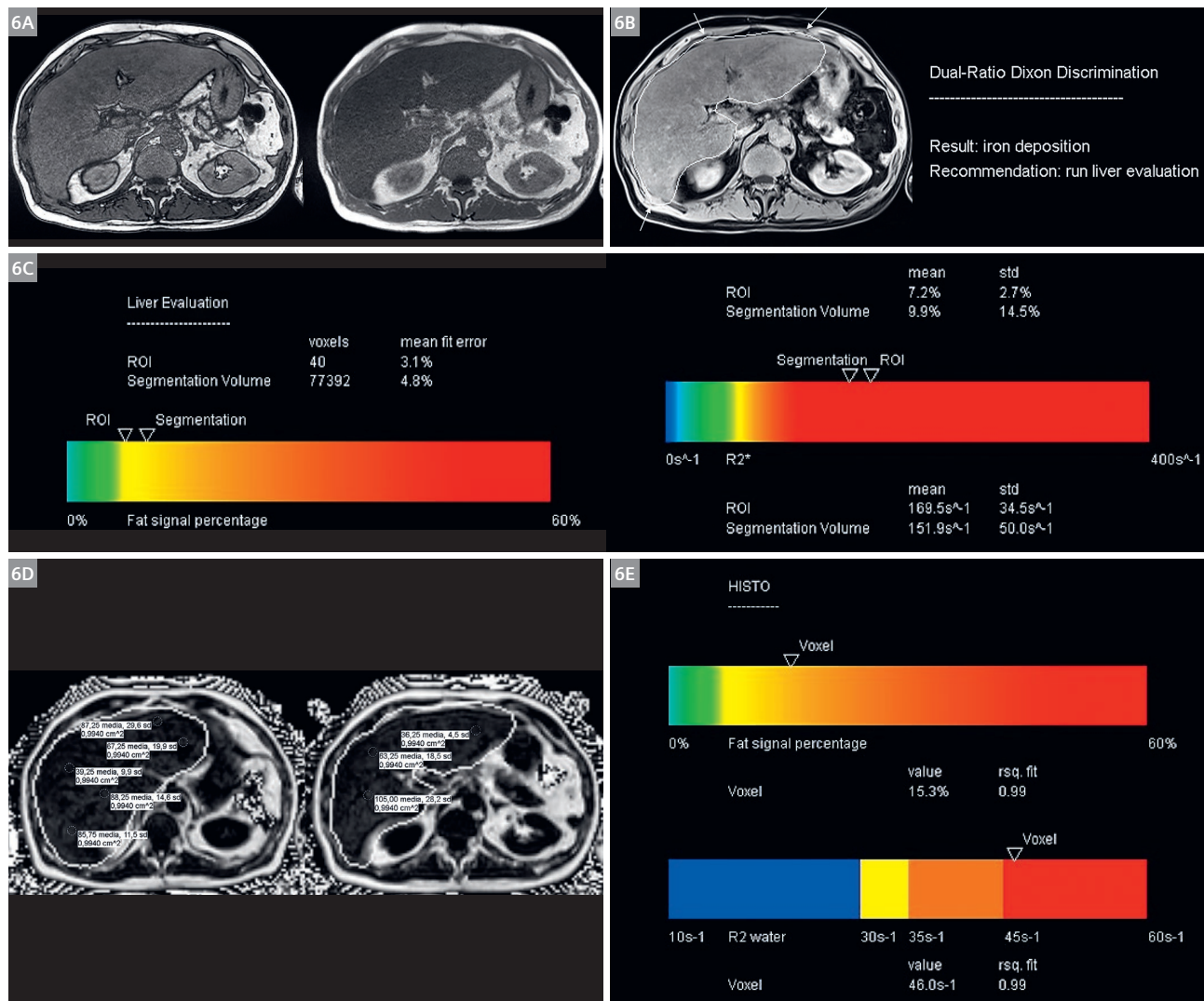
During postprocessing, PDFF and R2* can also be measured in each desired voxel of the liver, by placing the region of interest (ROI) in the most interesting hepatic segments in the FF and effective R2* series. In this way an estimate of steatosis can be made for each part or lobe, which is useful if the patient must undergo liver resection [9].

The FF value multiplied by 10^{-1} corresponds to the PDFF value in that location. This makes it possible to classify steatosis in a very accurate manner: grade 0 (normal liver PDFF: 0–5%), grade 1 (mild PDFF: 5–17%), grade 2 (moderate PDFF: 17–22%), and grade 3 (severe PDFF: ≥ 22%).

The effective R2* is measured in Hertz (or sec^{-1}) and correlates to the value of LIC (liver iron concentration) through a specific conversion factor for each device. The LIC is the ratio of intrahepatic iron to the dry weight of the parenchyma. Normal LIC is < 1.8 mg/g (dry weight). Values between 3 and 7 indicate a mild iron overload, > 7 moderate, and > 15 severe. A LIC value of 7 mg/g is an indication for chelation therapy in patients with iron overload due to repeated blood transfusions [10–12].

Case 6
66-year-old male with recent detection of liver cirrhosis; no viral causes were documented and the patient denied any alcohol abuse. NASH-related cirrhosis was suspected, so LiverLab evaluation was requested.

6 **(6A)** T1 GRE in/opp sequences: the signal intensity of liver parenchyma is low in both series of images, especially in-phase.
(6B) e-Dixon liver segmentation is not perfect (arrows) because of low signal intensity of the parenchyma, but it can only influence segmentation volume values of PDFF and R2* at q-Dixon acquisition, but not ROIs measurements of these parameters.
(6C) q-Dixon report confirms PDFF = 7–10% (mild steatosis but with heterogeneous distribution) and R2* = 169.5 sec^{-1} corresponding to LIC of 5.44 mgFe/g (mild iron overload).
(6D) q-Dixon FF sequence: multiple ROIs in right and left lobes confirm very heterogeneous PDFF values, ranging between 4% and 10%.
(6E) HISTO acquisition report confirms iron overload (R2 water 46 sec^{-1}; normal values <30 sec^{-1}) in the single voxel measured in right lobe. PDFF is 15% in the same voxel.

The HISTO spectroscopy sequences are multi-echo sequences corrected for the T2 signal, at high speed, acquired on a single voxel. These sequences are based on the principle that there is a strong nonlinear correlation between the water R2 signal and the iron concentration, independent of the lipid concentration. The sequence contains an algorithm that integrates the water and fat signal for each TE acquired, and can be used to obtain the values of fat fraction and water R2 [13].

Three localizer sequences define the location of the voxel, and then an apnea sequence of about 18–20 seconds returns a spectrum of the shorter TEs to perform quality control of the values obtained at TE = 12 seconds, where two distinct peaks must be appreciated: water and fat. The sequence also shows the measured values of fat fraction and R2 water on color bars. If desired, the acquisition can be repeated in another voxel of your choice.

A T2* colored map can also be obtained by acquiring multi-echo T2* sequences.

Conclusion

These cases show how LiverLab can give a wealth of information to clinicians, useful for diagnosis, management and follow-up of patients with fat and/or iron liver overload. With its rapid acquisition (5–7 minutes) it can easily be integrated in a standard liver MRI protocol. Radiologists' skills in using and interpreting LiverLab acquisitions and measurements can improve rapidly once these sequences are added to the standard protocol in patients with hepatopathy. In our experience clinicians appreciate the information given about fat and/or iron liver overload, and ask for this type of evaluation more and more frequently.

Contact

Barbara Frittoli, M.D.
Radiologia 1 ASST-Spedali Civili di Brescia
p.le Spedali Civili 1
25123 Brescia
Italy
bfrittoli@gmail.com

References

1 Xiaozhou M, Nagaraj-Setty H, Kambadakone R, Kenudson-Mino M, Hahn PF, Sahani DV. Imaging based Quantification of Hepatic Fat: Methods and Clinical Applications. RadioGraphics. 2009;29(5):1253-1280.

2 Caussy C, Reeder SB, Sirlin CB, Loomba R. Noninvasive, Quantitative Assessment of Liver Fat by MRI-PDFF as an Endpoint in NASH Trials, Hepatology. 2018;68(2):763-772.

3 Mouzaki M, Trout AT, Arce-Clachar AC, Bramlage K, Kuhnell P, Dillman JR et al. Assessment of Nonalcoholic Fatty Liver Disease Progression in Children Using Magnetic Resonance Imaging. The Journal of Pediatrics. 2018;201:86-92.

4 Yu EL, Golshan S, Harlow KE, Angeles JE, Durelle J, Goyal NP et al. Prevalence of Nonalcoholic Fatty Liver Disease in Children with Obesity. The Journal of Pediatrics. 2018; in press, available online since 14 Dec 2018 from https://www.sciencedirect.com/journal/the-journal-of-pediatrics/articles-in-press.

5 Deng J, Zhong X, Fishbein M et al. Hepatic Fat Quantification in Pediatric Patients using Multi-echo Dixon VIBE: Early Experience. MAGNETOM Flash. 2015;2(62):23-25.

6 Hutton C, Gyngell ML, Milanesi M, Bagur A, Brady M. Validation of a standardized MRI method for liver fat and T2 quantification. PLoS ONE. 2018;13(9):e0204175. https://doi.org/10.1371/journal.pone.0204175

7 Sharma P, Martin D. An Efficient Workflow for Quantifying Hepatic Lipid and Iron Deposition using LiverLab. MAGNETOM Flash. 2014;3(58):12-17.

8 Sellers R. MR LiverLab. MAGNETOM Flash. 2016;3(66):39-43.

9 Kim HJ, Cho HJ, Kim B, You MY, Lee JH, Huh J et al. Accuracy and precision of proton density fat fraction measurement across field strengths and scan intervals: A phantom and human study. Journal of Magnetic Resonance Imaging. 2018; in press, available online since 14 Nov 2018 from https://onlinelibrary.wiley.com/toc/15222586/0/0

10 Wood JC. Use of magnetic resonance imaging to monitor iron overload. Hematol Oncol Clin North Am. 2014;28(4):747-64.

11 Henninger B, Zoller H, Rauch S, Finkenstedt A, Shocke M, Jaschke W et al. R2* relaxometry for the quantification of hepatic iron overload: biopsy based calibration and comparison with the literature. RoFo. 2015;187(6): 472-479.

12 Quinn C, St Pierre T. MRI Measurements of Iron Load in Transfusion-Dependent Patients: Implementation, Challenges, and Pitfalls. Pediatr Blood Cancer. 2016;63:773–780.

13 Reeder SB, Cruite I, Hamilton G, Sirlin CB. Quantitative assessment of liver fat with magnetic resonance imaging and spectroscopy. J. Magn. Reson. Imaging. 2011;34:729-749.

14 Pineda N, Sharma P, Qin Xu, Hu X, Vos M, Martin DR. Measurement of Hepatic Lipid: High-Speed T2-Corrected Multiecho Acquisition at 1H MR Spectroscopy—A Rapid and Accurate Technique. Radiology. 2009;252(2):568-576. https://doi.org/10.1148/radiol.2523082084.